

1 **Measurement of longitudinal single-spin**  
2 **asymmetries for  $W^\pm$  boson production in polarized**  
3  **$p + p$  collisions at  $\sqrt{s} = 510$  GeV at STAR**

---

**Devika Gunarathne**<sup>\*†</sup>

Temple University, Philadelphia, PA, USA

E-mail: [devika@temple.edu](mailto:devika@temple.edu)

$W^\pm$  boson production in longitudinally polarized  $p + p$  collisions provides unique and clean access to the individual helicity polarizations of  $u / d$  quarks and anti-quarks. Due to the maximal violation of parity in the coupling,  $W$  bosons couple to left-handed quarks and right-handed anti-quarks and hence offer direct probes of their respective helicity distributions in the nucleon. These can be extracted from measured parity-violating longitudinal single-spin asymmetries,  $A_L$ , for  $W^{+(-)}$  boson production as a function of the decay lepton (positron) pseudo-rapidity  $\eta$ . The STAR experiment is well equipped to measure  $A_L$  for  $W^\pm$  boson production for  $|\eta| < 1$ . The published STAR  $A_L$  results (2011 and 2012 data combined) have been used by several theoretical analyses suggesting a significant impact in constraining the helicity distributions of anti- $u$  and anti- $d$  quarks. In 2013 the STAR experiment has collected a large data sample of  $\sim 250 \text{ pb}^{-1}$  which is more than 3 times larger than the total integrated luminosity in 2012, at  $\sqrt{s} = 510$  GeV with an average beam polarization of  $\sim 54\%$ , comparable to run 2012. The status of the 2013  $A_L$  analysis will be discussed along with an overview of future plans.

*The XXIII International Workshop on Deep Inelastic Scattering and Related Subjects*

*April 27 - May 1, 2015*

*Southern Methodist University*

*Dallas, Texas 75275*

---

\*Speaker.

†for the STAR collaboration

## 4 1. Introduction

5 There has been steady progress over the past few decades in terms of understanding the spin  
6 structure of the nucleon, one of the fundamental questions in nuclear physics. In the 1980s, the spin  
7 of the proton was naively explained [1] by the alignment of spins of the valence quarks. However,  
8 in our current understanding [2], the valence quarks, sea quarks, gluons and their possible orbital  
9 angular momentum are all expected to contribute to the overall spin of the proton. Despite this  
10 significant progress, our understanding of the individual polarizations of quarks and antiquarks is  
11 not yet complete. According to the spin sum rule introduced by Jaffe and Manohar [3] in 1990, the  
12 spin of the proton can be written in terms of its contributions from the intrinsic quark and antiquark  
13 polarization, intrinsic gluon polarization and their possible orbital angular momentum. Polarized  
14 inclusive deep-inelastic scattering (DIS) experiments were able to strongly constrain the total quark  
15 contribution to the proton spin [4]. However, DIS experiments were not sensitive to the flavor sep-  
16 arated individual quark spin contributions. These were then measured by polarized semi inclusive  
17 DIS experiments (SIDIS), but relatively large uncertainties were observed in the extracted helicity-  
18 dependent parton distribution functions (PDF) [4] of antiquarks compare to quarks. However, this  
19 method is limited by uncertainties in the fragmentation process [5]. The production of  $W^\pm$  bosons  
20 in longitudinally polarized  $p + p$  collisions at RHIC provides a unique and powerful tool to probe  
21 the individual helicity PDFs of light quarks and anti-quarks in the proton. Due to the maximal  
22 parity violating nature of the weak interaction,  $W^{-(+)}$  bosons couple to the left-handed quarks and  
23 right-handed anti-quarks and hence offer direct probes of their respective helicity distributions in  
24 the nucleon. These distributions can be extracted by measuring the parity-violating longitudinal  
25 single-spin asymmetry,  $A_L$ , as a function of the decay electron (positron) pseudo-rapidity,  $\eta_e$ . The  
26 longitudinal single-spin asymmetry is defined as  $A_L = (\sigma_+ - \sigma_-)/(\sigma_+ + \sigma_-)$ , where  $\sigma_{+(-)}$  is the  
27 cross section when the helicity of the polarized proton beam is positive (negative). At leading or-  
28 der,  $W^+ A_L$  is directly related to polarized anti d and u quark distributions ( $\Delta\bar{d}$ ,  $\Delta u$ ) while  $W^- A_L$  is  
29 directly related to polarized anti u and d quark distributions ( $\Delta\bar{u}$ ,  $\Delta d$ ) [6].

30 The results [7] of the single-spin asymmetries for  $W^\pm$  boson production in longitudinally  
31 polarized  $p + p$  collisions from the 2011 and 2012 STAR running periods are presented. The  
32 integrated luminosity of the data set collected during these two years were 9 and 77  $pb^{-1}$ , with  
33 an average beam polarization of 49% and 56%, respectively. In 2013 the STAR experiment has  
34 collected a data sample of  $\sim 250 pb^{-1}$  at  $\sqrt{s} = 510$  GeV with an average beam polarization of  
35  $\sim 54\%$ . The status of the 2013  $W A_L$  analysis is discussed.

## 36 2. Analysis

37 The STAR experiment [8] is well equipped to measure  $A_L$  for  $W^\pm$  boson production within  
38 a pseudorapidity range of  $|\eta| < 1$ .  $W^\pm$  bosons are detected via their  $W^\pm \rightarrow e^\pm \nu$  decay channels.  
39 A subsystem of the STAR detector, the Time Projection Chamber (TPC) is used to measure the  
40 transverse momentum ( $p_T$ ) of decay electrons and positrons and to separate their charge sign. Two  
41 other subsystems, Barrel and Endcap Electromagnetic Calorimeters (BEMC, EEMC) are used to  
42 measure the energy of decay leptons. A well developed algorithm [7] is used to identify and re-  
43 construct  $W^\pm$  candidate events by reducing large QCD type background events. In this algorithm,

44 various cuts are designed at each level of the selection process based on the kinematics and topo-  
 45 logical differences between the electroweak process of interest and QCD processes. For example,  
 46 tracks associated with  $W^\pm$  candidate events can be identified as isolated tracks in the TPC that  
 47 point to an isolated EMC cluster in the calorimeter, where as for QCD type events have several  
 48 TPC tracks point to several EMC clusters. In contrast to QCD background events, large opposite  
 49 missing transverse energy can be observed in  $W^\pm \rightarrow e^\pm \nu$  decay, due to undetected neutrinos. This  
 50 leads to a large imbalance in the vector  $p_T$  sum of all reconstructed final-state objects in W  
 51 candidate events, which is expressed as  $\vec{p}_T^{balance}$  in equation 2.1. Here  $\vec{p}_T^{jets}$  is determined using the  
 52 anti- $k_T$  algorithm [6]. A cone of radius of 0.7 in  $\eta - \phi$  space is centered around the candidate  
 53 lepton, and the  $p_T$  from all reconstructed jets outside of the cone are included. The  $\vec{p}_T^e$  is the  $p_T$  of  
 54 the candidate lepton. A strong correlation can be observed between  $E_T$  and scalar quantity, signed  
 55  $p_T$  balance, which is defined in equation 2.2. This can be seen clearly in Figure 1 c) which shows  
 56 the MC results simulating  $W^\pm \rightarrow e\nu$  decays. After initially requiring reconstructed TPC tracks to  
 57 have  $p_T > 10$  GeV, tracks are matched to a  $2 \times 2$  EMC cluster with transverse energy  $E_T > 12$  GeV.  
 58 W candidate events are then isolated using the large opposite missing energy requirement. This  
 59 is done by requiring that the  $E_T$  fraction of the  $2 \times 2 / 4 \times 4$  tower clusters is larger than 95%. The  
 60 final requirement, which is based on the large imbalance in the vector  $p_T$  sum mentioned above, is  
 61 signed- $p_T$  balance to be greater than 14 GeV, which is indicated by the red line in Figure 1 b). After  
 62 all the selection cuts have been applied, the characteristic Jacobian peak in the  $E_T$  distribution for  
 63 mid-rapidity  $W^\pm$  candidate events can be observed near half of the  $W^\pm$  mass, as shown in Figure 1  
 64 (a).

$$\vec{p}_T^{balance} = \vec{p}_T^e + \sum_{\Delta R > 0.7} \vec{p}_T^{jets} \quad (2.1)$$

65

$$signed\ p_T\ balance = \frac{(\vec{p}_T^e) \cdot \vec{p}_T^{balance}}{|\vec{p}_T^e|} \quad (2.2)$$

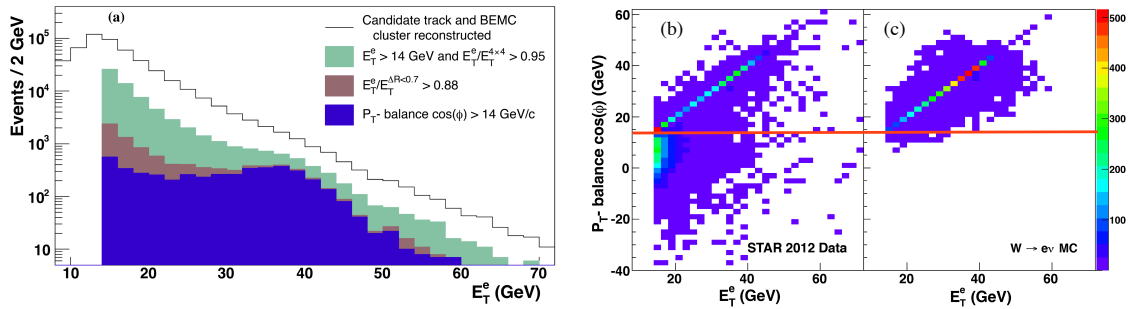


Figure 1: Candidate  $E_T^e$  distribution from the data after various selection cuts (a), Signed  $p_T$ -balance vs  $E_T^e$  for data (b) and  $W \rightarrow e\nu$  MC (c). [7]

66 The Charge separated  $W^\pm$  yields from the 2011 and 2012 data sets as a function of  $E_T^e$  are  
 67 shown in Figure 2 for different  $\eta$  bins, along with the estimated residual background contribu-  
 68 tions from  $W^\pm \rightarrow \tau^\pm \nu_\tau$ ,  $Z/\gamma^* \rightarrow e^+e^-$  electroweak processes and QCD processes. Relatively  
 69 small electroweak background contributions are estimated from Monte-Carlo (MC) simulation,  
 70 with PYTHIA 6.422 [9] generated events passing through the STAR GEANT[10] model and em-  
 71 bedded in to STAR zero-bias triggered events. Despite a significant reduction of QCD background  
 72 events during the selection process, a certain amount is still present in the signal region. This con-  
 73 tribution originates primarily from events which satisfy candidate  $W^\pm$  isolation cuts but contain  
 74 jets which escape the detection outside the STAR acceptance. Two procedures referred as "Second  
 75 EEMC" and "Data-driven QCD" [11], are used to estimated the background associated with the  
 76 acceptance ranges  $-2 < \eta < -1.09$  and  $|\eta| > 2$ . At forward rapidity, ( $1 < \eta_e < 1.4$ ), the W selec-  
 77 tion criterion used is similar to that of mid rapidity. The background estimation is improved using  
 78 additional Endcap Shower Maximum Detector (ESMD). More details are described in [7].

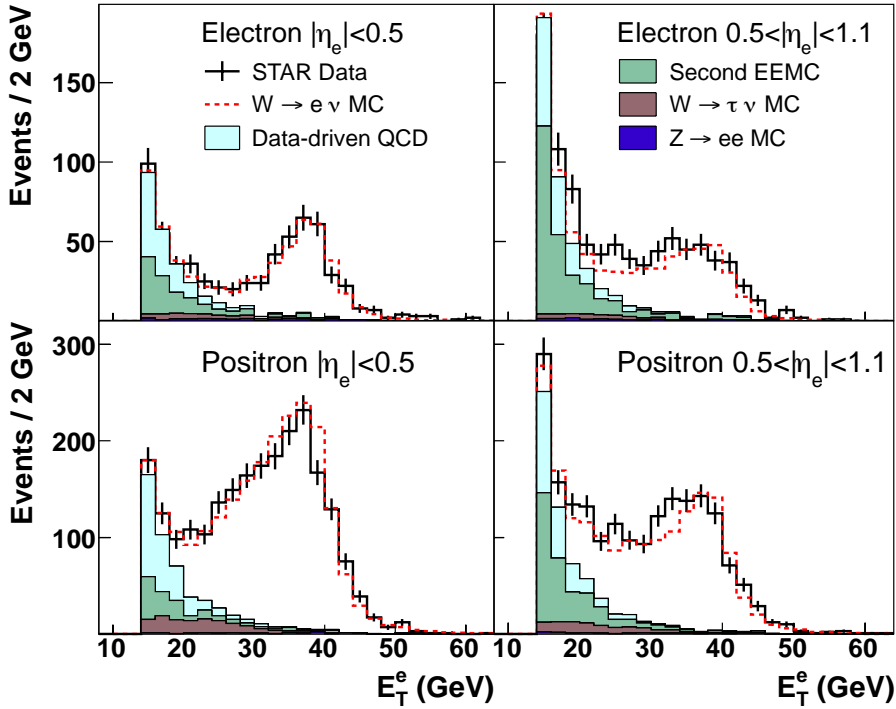


Figure 2:  $E_T^e$  distribution of  $W^-$  (top) and  $W^+$  (bottom) candidate events (black), various back-  
 ground contributions and sum of backgrounds and  $W \rightarrow e \nu$  MC signal (red-dashed). [7]

### 79 3. Results

80 To properly account for the low statistics in the 2011 data set, a profile likelihood method was  
 81 used to extract the spin asymmetry results from the combined 2011 and 2012 data sets. Two like-  
 82 likelihood functions  $L_{year1}$  and  $L_{year2}$  are defined for each of the 2011 and 2012 data sets respectively.  
 83 The asymmetry results, central values and confidence intervals are extracted from the product of the

84 likelihood function,  $L_{2011} \times L_{2012}$ . More details are described in [7]. The  $W^\pm$  single-spin asymme-  
 85 try results measured for  $e^\pm$  with  $25 < E_T^e < 50 \text{ GeV}$  are shown in Figure 3 as the function of decay  
 86  $e^\pm$  pseudorapidity,  $\eta_e$  in comparison to theoretical predictions based on DSSV08 [12] and LSS10  
 87 [13] helicity-dependent PDF sets, using both CHE (next-to-leading order) [6] and RHICBOS (fully  
 88 resummed) frameworks [14]. The measured  $A_L^{W^-}$  is larger than the central value of the theoretical  
 89 predictions. The enhancement at large negative  $\eta_e$ , in particular is sensitive to the polarized anti  
 90 u quark distribution,  $\Delta\bar{u}$ .  $A_L^{W^+}$  is negative as expected and consistent with theoretical predictions.  
 91 The systematic uncertainties for  $A_L^{W^\pm}$  are well under control for pseudorapidity range  $|\eta_e| < 1.4$ .  
 92 STAR 2012 preliminary  $A_L^{W^\pm}$  results [4] are included in the DSSV++ global analysis [15] from the  
 93 DSSV group and recent NNPDF [16] global analysis. Both analyses show that the STAR  $W A_L$   
 94 results provide a significant constraint on anti u ( $\Delta\bar{u}$ ) and anti d ( $\Delta\bar{d}$ ) quark polarizations.

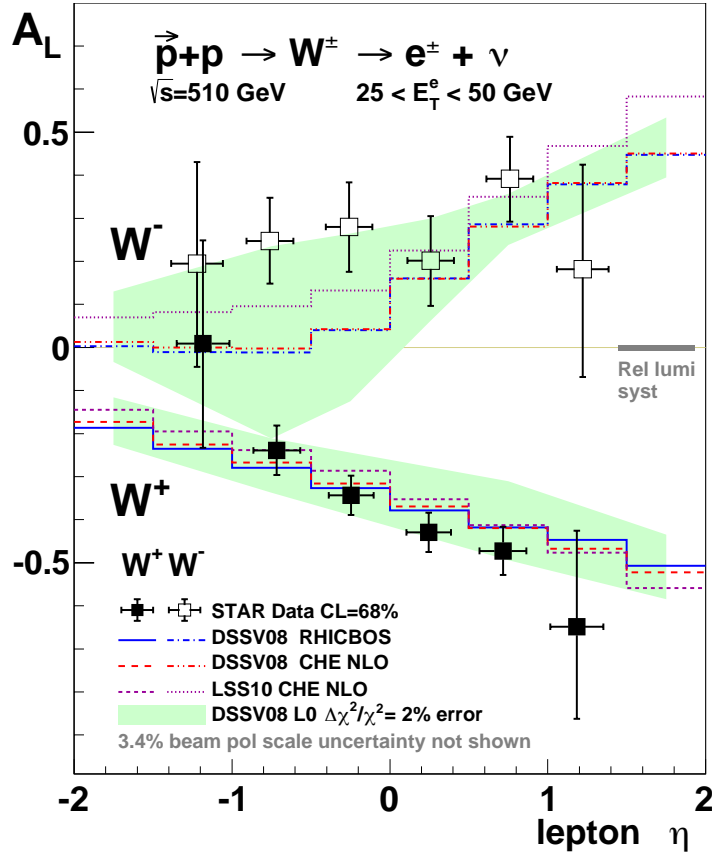


Figure 3: Longitudinal single-spin asymmetries for  $W^\pm$  production as a function of lepton pseudo-rapidity,  $\eta_e$  in comparison to theory predictions. [7]

#### 95 4. Outlook

96 In 2013, the STAR experiment collected a large data sample of  $\sim 250 \text{ pb}^{-1}$ , which is more  
 97 than 3 times larger than the total integrated luminosity in 2012, at  $\sqrt{s} = 510 \text{ GeV}$  with an average  
 98 beam polarization of  $\sim 54\%$ . The high luminosity data collected in 2013 require proper calibration

99 of all the subsystems used in the analysis. As the charge sign reconstruction of  $e^+$  and  $e^-$  is based  
 100 on the bending of TPC tracks in the presence of an axial magnetic field, the calibration of the TPC  
 101 is crucial for the  $W$  analysis. Despite the challenging environment in the calibration process due  
 102 to large pile up accumulated in the TPC due to high luminosity  $p + p$  collisions in 2013, a clear  
 103 separation between  $e^+$  and  $e^-$  is observed. The calibration of the other crucial subsystem for the  
 104 mid-rapidity  $W$  analysis, the BEMC, is currently in progress. Forward Gem Tracker (FGT) was  
 105 fully installed at STAR in year 2013, which covers the acceptance between  $1 < \eta < 2$  in the forward  
 106 region. The FGT will be used as the tracking device for  $W$  analysis in the forward pseudorapidity  
 107 region at STAR. This enhances the sensitivity to  $\bar{u}$  and  $\bar{d}$  quark polarizations. Figure 4 shows the  
 108 projected uncertainties for the  $W^\pm$  asymmetries estimated from the 2013 data set.

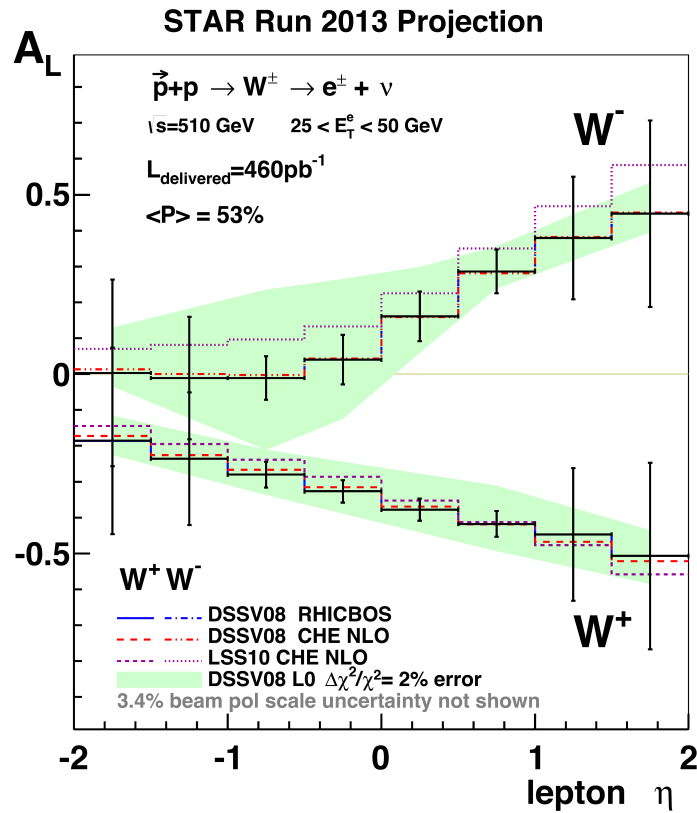


Figure 4: Projected uncertainties for the longitudinal single-spin asymmetries as a function of lepton pseudorapidity,  $\eta_e$  for  $W^\pm$  production from the 2013 data set.

109 Higher precision results are expected from the STAR 2013  $W A_L$  analysis to improve con-  
 110 straints on the sea quarks helicity-dependent PDFs.

111 **References**

112 [1] J. R. Ellis and R. L. Jaffe, A Sum Rule for Deep Inelastic Electroproduction from Polarized Protons,  
 113 Phys. Rev. **D9**, 1444 (1974).

- 114 [2] European Muon Collaboration, J. Ashman *et al.*, Phys. Rev. Lett. **B206**, 364 (1988).
- 115 [3] R. Jaffe and A. Manohar, The G(1) Problem: Fact and Fantasy on the Spin of the Proton, Nucl. Phys.  
116 **B337**, 509 (1990), revised version.
- 117 [4] D. de Florian, R. Sassor, M. Stratmann, and W. Vogelsang, Extraction of Spin-Dependent Parton  
118 Densities and Their Uncertainties, Phys. Rev. **D80**, 034030 (2009).
- 119 [5] B. Adeva *et al.*, (Spin Muon Collaboration), Polarized quark distributions in the nucleon from semi  
120 inclusive spin asymmetries, Phys. Lett. **B420**, 180 (1998).
- 121 [6] D. de Florian and W. Vogelsang, Helicity parton distributions from spin asymmetries in W-boson  
122 production at RHIC, Phys. Rev. **D81**, 094020 (2010).
- 123 [7] STAR Collaboration, L. Adamczyk *et al.*, Phys. Rev. Lett. **113**, 072301 (2014).
- 124 [8] K.H. Ackermann *et al.*, Nucl. Instrum. Meth. **A 499**, 624 (2003)
- 125 [9] T. Sjostrand, S.Mrenna, and P.Z. Skands, PYTHIA 6.4 Physics and Manual, JHEP **05**, 026 (2006).
- 126 [10] R. Brun *et al.*, GEANT: Simulation Program for Particle Physics Experiments. User Guide and  
127 Reference Manual, CERN-DD-78-2-REV (1978).
- 128 [11] STAR Collaboration, L. Adamczyk *et al.*, Phys. Rev. **D85**, 092010 (2012).
- 129 [12] D. de Florian, R. Sassor, M. Stratmann, and W. Vogelsang, Phys. Rev. Lett. **101**, 072001 (2008).
- 130 [13] E. Leader, A. V. Sidorov, and D. B. Stamenov, Determination of polarized parton densities from a  
131 QCD analysis of inclusive and semi-inclusive deep inelastic scattering data, Phys. Rev. **D82**, 114018  
132 (2010).
- 133 [14] P. M. Nadolsky and C. Yuan, Nucl. Phys. **B666**, 31 (2003)
- 134 [15] E. Aschenauer *et al.*, (2013), arXiv:1304.0079 [nucl-ex].
- 135 [16] E.R. Nocera, arXiv:1403:0440 [hep-ph] (2014).